Hydrogen-Bonding Interactions at the Vapor/Water Interface Investigated by Vibrational Sum-Frequency Spectroscopy of $HOD/H_2O/D_2O$ Mixtures and Molecular Dynamics Simulations

Elizabeth A. Raymond, Teresa L. Tarbuck, Mac G. Brown,§ and Geraldine L. Richmond*

Department of Chemistry and Materials Science Institute, University of Oregon, Eugene, Oregon 97403

Received: June 6, 2002; In Final Form: September 19, 2002

Vibrational sum-frequency spectroscopy (VSFS) studies of a series of $HOD/H_2O/D_2O$ mixtures ranging from pure D_2O to pure H_2O have been performed at the vapor/water interface. The various concentrations allow an iterative fitting procedure to be applied, resulting in a set of resonant peaks which consistently describe the vibrational modes of water molecules present in the interfacial region. The resonant sum-frequency response from the contributing vibrational modes allows more definitive characterization than in previous studies of the bonding interactions between surface water molecules. Comparison of the resonant spectrum of the vapor/H_2O interface with the sum-frequency spectrum obtained at the CCl_4/H_2O interface reveals more similarity between the interfacial hydrogen-bonding environments than previously determined. Recent molecular dynamics simulations of VSF spectra of the vapor/H_2O interface are in good agreement with the experimentally obtained spectra, and give insight into the molecular interactions in the interfacial region, as well as an estimate of the interfacial depth probed.

Introduction

Surfaces and interfaces play important roles in almost every aspect of our surrounding world, from droplets in the atmosphere, to cell membranes, to materials leaching through soils. However, despite their pervasiveness, the fundamental chemistry and physics occurring at interfaces is not well understood. Perhaps the most simple of these interfaces, the vapor/water interface, has been investigated using many experimental techniques, but the molecular interactions in the interfacial region are still not well characterized. One such surface specific technique which has been used in recent years has been vibrational sum-frequency spectroscopy (VSFS).[1−4] VSFS is an inherently surface specific technique which provides vibrational spectra of those molecules that are influenced by the presence of the interface.

The broad OH stretching intensity observed in IR and Raman spectra of liquid water demonstrates the wide variety of hydrogen-bonding environments experienced by water molecules. While bulk water systems have been extensively studied both experimentally as well as theoretically, the structure at the vapor/water interface remains less well understood than in the bulk. The pioneering studies of the Shen laboratory obtained the first vibrational spectra of the liquid water surface and explored its temperature dependence.[5,6] However, the broad OH stretching band observed, coupled with the inherent complexity of vibrational sum-frequency spectra, did not allow a very detailed description of the hydrogen-bonding environment present in the interfacial region to be formed. An exception to this was the characterization of the dangling OH stretch at $\sim$3700 cm^{-1}. This vibrational mode, which arises from the stretching of an OH oscillator protruding into the vapor phase that does not participate in hydrogen bonding, is energetically well separated from the other OH stretching modes in the spectrum and is therefore more easily analyzed. The vapor/water interface was found to be composed of at least 20% free OH oscillators, and an average orientation angle of $\sim$38° from the surface normal was calculated.[5,6] The hydrogen-bonding environment was characterized as being "ice-like" in nature, based on the significant intensity observed in the lower frequency (3100−3300 cm^{-1}) region of the spectrum.[7]

As with bulk studies of liquid H_2O, the broad nature of the vibrational resonances makes characterization of the hydrogen-bonding environments difficult without further experiments which allow deconvolution of the spectrum into its individual components. To achieve this, we have performed isotopic dilution experiments, which by forming HOD, remove the intramolecular coupling between the two oscillators, thereby simplifying the OH stretching region of the spectrum. Collecting spectra of different concentration HOD, H_2O, and D_2O mixtures has also provided a set of constraints for fitting the spectra, enabling a more detailed description of the hydrogen-bonding environment in the interfacial region to be obtained. This paper expands upon both the data and analysis of these mixtures presented in a previous letter.[8] In addition to the conclusions obtained from the detailed isotopic dilution studies, recent MD simulations performed by Morita and Hynes[9,10] as well as in our laboratory, have been used to calculate sum-frequency spectra of the vapor/H_2O interface. Given the similarity of the calculated spectra to the experimentally obtained spectra, these simulations allow for further investigation of the molecular orientations and interactions occurring in the interfacial region.

SF Background and Analysis

Vibrational sum-frequency spectroscopy is a second-order nonlinear optical technique that provides a vibrational spectrum of the molecules present at the interface between two media. The sum-frequency intensity which is detected in these experi-

* Author to whom all correspondence should be addressed.
§ Present address: Los Alamos National Lab, Los Alamos, NM, 87545.

10.1021/jp021366w CCC: $25.00
Published on Web 12/18/2002

ments is proportional to the square of the second-order polarization induced in the interfacial molecules by the overlap of a visible and a tunable infrared laser beam.[2,11−15] This second-order polarization is proportional to the electric fields transmitted through the interface, $\mathbf{f}_{Vis}\mathbf{E}_{Vis}$, and $\mathbf{f}_{IR}\mathbf{E}_{IR}$, and the macroscopic response of the interfacial molecules to the incident fields, $\chi^{(2)}$.

$$I_{SF} \propto |\mathbf{P}^{(2)}|^2 \propto |\mathbf{F}_{SF}\chi^{(2)}:\mathbf{f}_{Vis}\mathbf{E}_{Vis}\mathbf{f}_{IR}(\mathbf{n}_{H_2O})\mathbf{E}_{IR}|^2 \qquad (1)$$

$\mathbf{F}_{SF}$, $\mathbf{f}_{Vis}$, and $\mathbf{f}_{IR}$ are the nonlinear and linear Fresnel coefficients, respectively. The nonlinear susceptibility, $\chi^{(2)}$, consists of both a resonant and a nonresonant response.

$$\chi^{(2)} = \chi^{(2)}_{NR} + \sum_{\nu}\chi^{(2)}_{\nu} \qquad (2)$$

In general, the nonresonant nonlinear susceptibility is small for liquid surfaces,[2] but as is shown by these experiments, is non-negligible for a vapor/water interface. The resonant sum-frequency response is a sum of resonant peaks, which can each be described by eq 3.

$$\chi_{\nu}^{(2)} = \int_{-\infty}^{\infty} \frac{\mathbf{A}_{\nu} e^{-[(\omega_L-\omega_{\nu})/\Gamma_{\nu}]^2}}{\omega - \omega_L - i\Gamma_L}\, d\omega_L \qquad (3)$$

This expression, first used by Bain,[11] convolves the homogeneous line width of the transition, (HWHM, Γ_L), with the inhomogeneous broadening (FWHM, $\sqrt{2\ln 2}\ \Gamma_{\nu}$) arising from the multitude of molecular environments present in the condensed phase. $\mathbf{A}_{\nu}$, a complex quantity, can be thought of as the total sum-frequency transition strength, as it is proportional to the product of the number of molecules probed and the orientationally averaged IR and Raman transition moments for the molecules contributing to the SF signal.

The spectra of H_2O containing solutions presented here are fit using the amplitude of the nonresonant response obtained from the pure D_2O spectrum, and four resonant peaks, which will be assigned and described in more detail later. Thus, the intensity observed in each spectrum is fit to the following expression:

$$I_{SF} \propto |\chi^{(2)}_{NR} + \chi^{(2)}_{1R} + \chi^{(2)}_{2R} + \chi^{(2)}_{3R} + \chi^{(2)}_{4R}|^2 \qquad (4)$$

where each $\chi^{(2)}$ element has an amplitude and a phase. Once the best fit to each spectrum is obtained, the resonant and nonresonant responses can be separated, so that the molecular interpretation of the interfacial region is based solely on the resonant sum-frequency response.

Spectral Fitting

Spectra of H_2O containing solutions in the OH stretching region, where several broad overlapping peaks contribute to the spectral intensity, are difficult to deconvolve for even linear spectroscopic techniques. This common difficulty, when combined with the number of peak parameters that contribute to a sum-frequency spectrum, makes fitting sum-frequency spectra a challenging task. Each spectral peak included in a fit has a Lorentzian and a Gaussian width, a center frequency, an amplitude and a phase. To make this a tractable problem, the spectra of differing mixtures of HOD, H_2O, and D_2O are fit iteratively to produce a set of global peak parameters, such that the Gaussian widths, phases, and central frequencies are consistent for each peak throughout the entire concentration series, with the exception of the free OH peak, which will be discussed in a later section. This iterative fitting procedure allows the sum-frequency spectra of H_2O containing solutions to be fit with only four resonant peaks. When unconstrained by other spectral fits, the neat H_2O spectrum can be fit equally well with between three and six peaks, due to the number of free parameters, while the spectrum containing primarily HOD in D_2O can be fit with between two and four peaks. The iterative fitting procedure, which requires all five spectra to have the same contributing peaks, constrains each fit to four resonant peaks, which change only in amplitude throughout the concentration series (again, with the exception of the free OH).

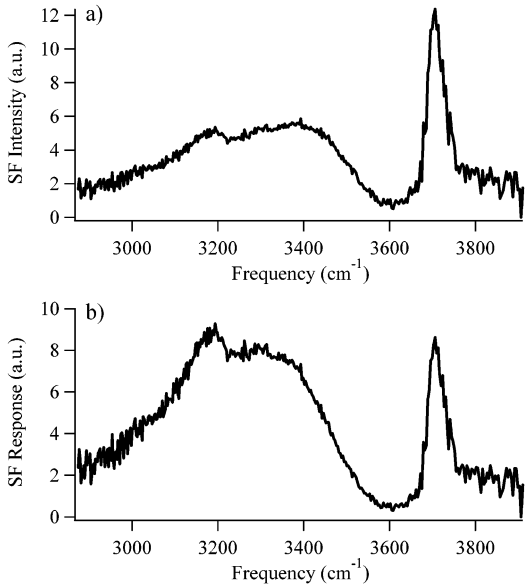

Figure 1. (a) VSF spectrum of the vapor/H_2O interface, after normalization by the SF spectrum of ⟨100⟩ GaAs. (b) Vapor/H_2O spectrum from Figure 1a, after correction by the linear and nonlinear Fresnel coefficients, including the dispersion in the index of refraction of H_2O as a function of frequency.

In addition to fitting the spectra iteratively, several assumptions were made in the fitting of the spectra to reduce the number of free parameters. The Lorentzian widths of the peaks, Γ_L, which are related to the homogeneous line widths of the transitions, were set to be 5 cm^{-1} for all peaks except the free OH, which was assigned a Γ_L value of 12 cm^{-1}. These values are based on measured relaxation rates for H_2O.[16,17] The other assumption which was applied was to constrain the phases of the peaks to be either 0° or 180°. This constraint on the relative phases, while likely the largest source of error in the fitting procedure, does not completely remove the orientation information which is encoded in the phase of the sum-frequency light, but does limit it. For the studies presented here, the free OH was chosen to have a phase of 0°, as it has an average orientation away from the bulk, so all other phases are relative to this zero point. In the case of a vapor/water interface, assuming that the observed vibrational modes are all of A_1 symmetry (little or no contribution from the asymmetric stretch), molecules or oscillators which have opposite orientations with respect to the surface plane will have opposite phases, that is, phases separated by 180°.[18]

While the spectrum of neat D_2O in the OH stretching region provides the magnitude of the nonresonant response, the phase cannot be determined from this spectrum alone. However, because the resonant response in the OH stretching region is smaller than the nonresonant response from a vapor/primarily HOD in D_2O interface, (Figure 2b) this spectrum can be used to obtain the relative phase relationship between the resonant

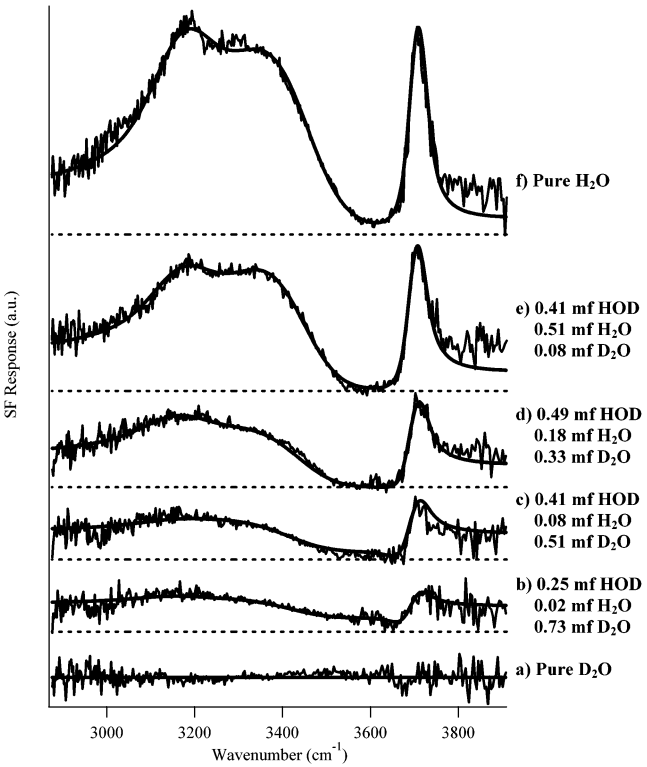

Figure 2. Offset VSF spectra of mixtures of H_2O, HOD, and D_2O, from pure D_2O (bottom) to pure H_2O (top). Equilibrium mole fractions (mf) are listed to the right of each spectrum. The D_2O spectrum has not been offset from the frequency axis which represents zero intensity. The zero signal levels of the remaining spectra are represented by the horizontal dashed lines. The best fits to the spectra are overlaid on the data as thick solid lines.

free OH response and the nonresonant response. The phase constraint of 0° or 180° for the nonresonant response relative to the resonant free OH response was removed when fitting this primarily HOD spectrum and resulted in a phase within one standard deviation of 180°, thereby justifying setting it to 180°.

Experimental

The laser system used in these experiments has been thoroughly described in previous publications,[19,20] but a brief description is warranted here. The light is generated from a amplified Ti:sapphire system which produces 2 ps pulses of 800 nm light at a repetition rate of 1 kHz. Approximately 200 μJ of this light is used as the visible beam, while the remaining 800 nm light is used with an OPG stage and two OPA stages to produce ~4−13 μJ of tunable IR between 2700 and 4000 cm^{-1}. The visible and infrared beams are combined on the surface in a collinear geometry, and the reflected sum-frequency is collected in a reflection geometry on a thermoelectrically cooled CCD camera. All of the spectra presented here are taken under *ssp* (sum-frequency, visible, IR) polarization conditions, where *s* and *p* denote polarizations parallel and perpendicular to the plane of incidence, respectively. This polarization combination probes dipole moments with a component perpendicular to the interface, and Raman polarizabilities with components parallel to the interfacial plane.

The samples are fully enclosed in a Teflon and glass cell with CaF_2 input and exit windows under an atmosphere of dry N_2(g). The H_2O used is obtained from a Millipore Nanopure system (17.9 MΩ cm), while the D_2O is "ultra low conductivity" (0.4 MΩ cm), purchased from CDN Isotopes. The liquids are introduced to the cell via "gastight" syringes to minimize contamination and maintain isotopic concentrations. All spectra are taken at room temperature (~21 °C) and atmospheric pressure.

Due to the interaction of the infrared beam with water vapor in the air, the 2 ps IR pulses are considerably lengthened in the ~3600−3800 cm^{-1} spectral region, resulting in a reduction in the amount of SF signal generated. To correct for this temporal de-phasing of the IR light, as well as for changes in the intensity of the IR beam as a function of frequency, the SF spectra presented here have been divided by the nonresonant SF spectrum of ⟨100⟩ GaAs. Due to the crystal structure of the GaAs, this SF signal arises from the bulk material,[21] and should be constant across the spectral region probed here. The spectrum of neat H_2O, which is obtained after normalization by GaAs (Figure 1a), is very similar to the most recent vapor/water sum-frequency spectrum obtained by the Shen laboratory.[22] The spectrum of the neat vapor/H_2O interface presented here is not compared to that obtained by the Shultz laboratory,[4] as their experiments were performed at ~0 °C, whereas our experiments are performed at room temperature.

The spectra presented here have been further corrected by dividing out the appropriate linear and nonlinear Fresnel coefficients[15] from the spectra, leaving a quantity which is proportional to only the square of the molecular response, $|\sum \chi^{(2)}|^2$, and is not dependent on the experimental geometry. This has been done to correct for the anomalous dispersion in the index of refraction of H_2O (and HOD) in the OH stretching region. Figure 1b shows the neat vapor/H_2O spectrum after division by the Fresnel coefficients. The index of refraction of HOD as a function of wavelength is unavailable, so weighted averages (using the initial concentrations of H_2O and D_2O) of the indices of H_2O and D_2O[23,24] were used to approximate the index of HOD-containing solutions. The improvements in the normalization procedures described above as well as in the laser system have resulted in a larger free OH response than previously measured in this laboratory.[18,19]

Results and Discussion

Figure 2 shows a series of offset sum-frequency spectra with progressively increasing initial concentrations of H_2O from pure D_2O (bottom) to pure H_2O (top). The pure D_2O spectrum has not been offset from the horizontal axis, which represents zero SF intensity, while the horizontal dotted lines represent the zero intensity values of the other spectra. The spectrum of D_2O is featureless, but nonzero, indicative of a purely nonresonant sum-frequency response, as D_2O has no vibrational resonances in the OH stretching region. The nonresonant response for all of the spectra presented in this work is assumed to have the same amplitude as that observed in the neat D_2O spectrum. The calculated equilibrium concentrations of H_2O, HOD, and D_2O are given alongside each spectrum, and assume an equal partitioning of hydrogen and deuterium to the surface. This assumption of equal partitioning is appropriate given the recent measurement of the difference in energy between a free OH and a free OD at the surface of ~52 cm^{-1},[25] which is considerably smaller than the available thermal energy (~203 cm^{-1}) at room temperature.

As the number of OH oscillators in the solution increases, (spectra b−f), the intensity in both the 3100−3450 and 3700 cm^{-1} regions of the spectra increases above the nonresonant level observed in the neat D_2O spectrum. In the region from ~3500−3650 cm^{-1}, the intensity dips below the observed nonresonant intensity. This decrease in intensity is indicative

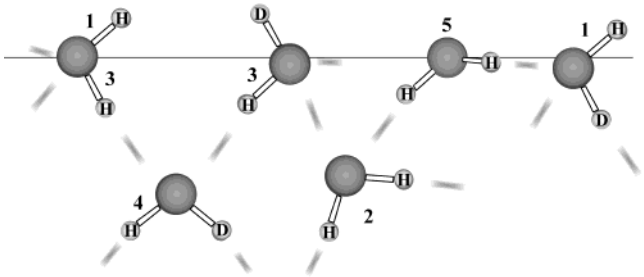

Figure 3. Schematic representation of the species expected at the vapor/HOD interface. The OH bonds are labeled as follows: (1) Free OH in a H_2O or HOD molecule. (2) Tetrahedrally coordinated H_2O molecule. (3) Uncoupled donor OH of a molecule containing a free OH or OD. (4) Uncoupled donor OH of a tetrahedrally coordinated HOD molecule. (5) Double donor H_2O molecule.

of interferences between the SF light arising from the resonant and nonresonant responses, and will be discussed in detail later. The relatively narrow spectral feature at ~3700 cm^{-1} is attributed to the stretching of uncoupled OH oscillators (from either H_2O or HOD) which protrude into the vapor phase and do not participate in hydrogen bonding (labeled as 1 in Figure 3). This interfacial species is most commonly referred to as the dangling or free OH. Due to the broad nature of the intensity in the 3100−3450 cm^{-1} region of the spectrum, precise spectral assignments cannot be made without further analysis, but several interfacial species are expected to have spectral signatures in this region. Figure 3, which depicts the expected species, is provided as an aid to the discussion of the various contributing modes present at any moment at this dynamic interface. Contributions from the OH stretching of tetrahedrally coordinated water molecules in the interfacial region, (labeled as 2 in Figure 3) should appear with stretching frequencies from ~3150 cm^{-1} in IR and Raman studies of ice to ~3300−3500 cm^{-1} in liquid water.[26−29] In addition to the tetrahedrally coordinated H_2O molecules, the stretching mode of the uncoupled donor OH is expected to appear in this spectral region (labeled 3 and 4 in Figure 3). The uncoupled donor OH is an OH oscillator which participates in hydrogen bonding, but whose stretching mode is energetically uncoupled from the other vibration of the oscillator in the molecule (either on OD or free OH) due to either a difference in hydrogen bonding (labeled as 3 in Figure 3) or a difference in mass (labeled as 4 in Figure 3). While this vibrational mode should be present in every molecule that also contains a free OH, it has not been assigned in previous sum-frequency studies of the vapor/H_2O interface. In solutions containing both HOD and H_2O, the uncoupled donor OH can arise from three different types of molecules: the OH stretching mode of tetrahedrally coordinated HOD, or the OH stretching of a hydrogen-bonded molecule (either HOD or H_2O), where the other oscillator does not participate in hydrogen bonding. The nearly complete uncoupling of the two stretches by differences in mass or hydrogen bonding means that the uncoupled donor OH stretches from these three types of molecules are expected at similar frequencies.

The OH streching of surface H_2O molecules oriented such that hydrogen bonding occurs through both OH (or OD) bonds, but not through the lone pairs (designated as 5 in Figure 3), called "double donors" have been observed in ice and cluster work[30−33] at ~3550 cm^{-1}. Although is probable that such double donor molecules contribute to the sum-frequency spectra, there is no clear feature in either the HOD or H_2O spectra which can be assigned to this species. These SF experiments have been performed at room temperature, while the ice and cluster work examined very cold molecules, which given the significant

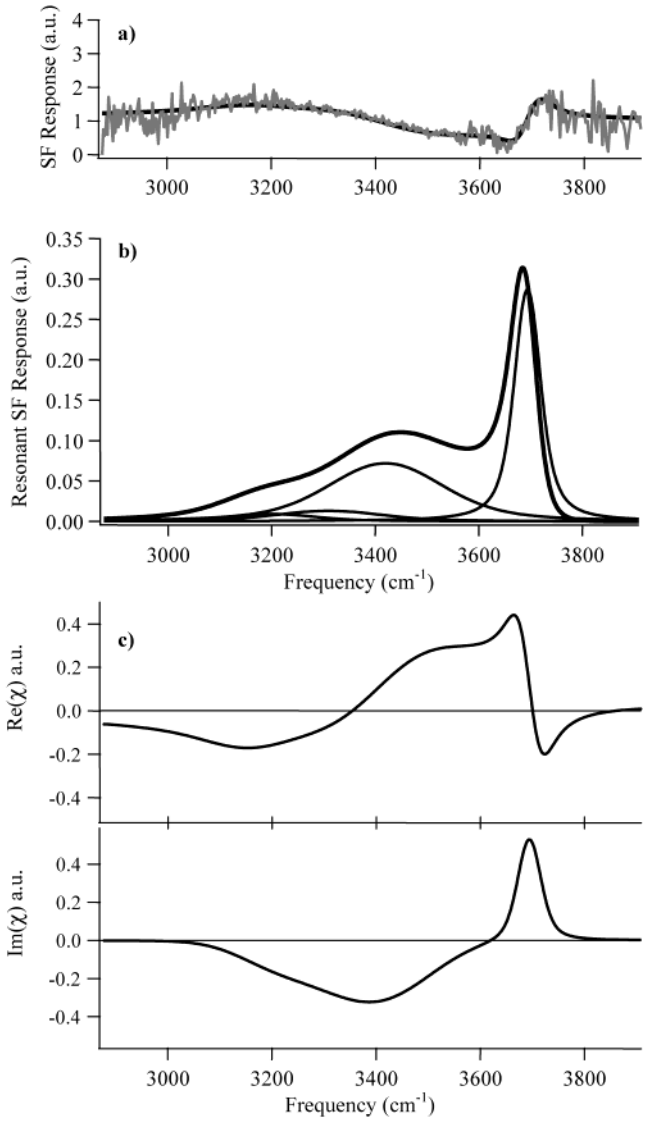

Figure 4. (a) Expanded VSF HOD spectrum (0.25 mf HOD, 0.02 mf H_2O, 0.73 mf D_2O) and fit. (b) Resonant SF response from interfacial HOD (thick solid line). The squared contributions from the different molecular species, $|\chi_\nu^{(2)}|^2$, are shown with thin solid lines. (c) Real and imaginary components of $\chi_\nu^{(2)}$ for a primarily HOD in D_2O interface.

temperature dependence of most OH stretches, places a large degree of uncertainty on where the double donor OH stretching should appear in a SF spectrum of room-temperature H_2O.

The spectral fits presented in Figure 2 can be deconvolved into their resonant and nonresonant components, and a molecular level interpretation of the hydrogen-bonding environments in the interfacial region can be deduced from this resonant sum-frequency response. The simplest spectrum to analyze in its component pieces is the spectrum with the highest ratio of HOD to H_2O (Figure 2b), as the resonant contributions to this spectrum arise primarily from the uncoupled OH stretches of HOD. An expanded spectrum and fit are shown in Figure 4a, whereas Figure 4b and 4c show different representations of the deconvolved resonant peaks. Figure 4c, which shows the real and imaginary components of the resonant susceptibility, $\sum_\nu \chi_\nu^{(2)}$, is useful for understanding how interferences between the spectral peaks create the unusual features observed in sum-frequency spectra, but does not provide direct insight into the molecular environments present in the interfacial region. Figure 4b is more useful for developing a molecular description of the

interfacial region, as it shows the square of the resonant contribution, $|\sum_\nu \chi_\nu^{(2)}|^2$, and the square of each individual resonant peak, $|\chi_\nu^{(2)}|^2$. The square of the total resonant contribution can be thought of as the sum-frequency spectrum in the absence of the nonresonant response arising from the interface, while the composite peaks give the peak positions, widths, and relative sizes. It is important to note that since the resonant sum-frequency intensity is proportional to the *square* of the number of contributing molecules, further analysis is required before number densities can be quantitatively compared, and appears in a later section.

After deconvolution of the resonant and nonresonant SF responses, the resonant SF response from the primarily HOD/D_2O interface (Figure 4b) can be more readily compared with bulk IR or Raman spectra than the spectrum shown in Figure 2b, although interferences still arise between the resonant modes where they overlap in frequency. Note, for example, the red shift of the free OH peak in the resonant spectrum in Figure 4b relative to the actual center frequency of the underlying peak assigned to the free OH. This shift is due to the overlap of the peaks centered at 3420 cm^{-1} and at 3694 cm^{-1}, and clearly demonstrates the need for careful analysis of sum-frequency spectra.

The resonant spectrum of the D_2O interface containing primarily HOD exhibits three significant intensity features: an intense free OH at ~3700 cm^{-1}, broad intensity centered at ~3420 cm^{-1}, and a smaller shoulder at ~3200 cm^{-1}. The frequency and width of the 3420 cm^{-1} peak match well with the spectral features observed in room-temperature IR studies of HOD in D_2O, and therefore this peak is assigned to the uncoupled donor OH. In IR studies of bulk HOD, this stretching band has been found to be temperature dependent, ranging in frequency from ~3200 cm^{-1} in studies of HOD ice to ~3400−3450 cm^{-1} in room-temperature HOD.[17,34,35] The peak frequency found here indicates that the hydrogen-bonding interactions being experienced by the uncoupled donor OH oscillators in the interfacial region are similar to those found in bulk HOD in liquid D_2O, that is they are characteristic of the hydrogen-bonding interactions found in a liquid. The two composite peaks that contribute to the shoulder of intensity in the resonant spectrum are centered at 3200 and 3310 cm^{-1}, and are assigned to tetrahedrally coordinated H_2O in the interfacial region, from the residual 0.02 mf H_2O in the solution. The amplitudes of these two peaks are large, given that only two percent of the solution is H_2O. This seemingly large amplitude is attributed to the increase in dipole transition strength that occurs as a result of increased hydrogen bonding,[36,37] thereby increasing the amount of sum-frequency light arising from each molecule.

As was discussed previously, the spectral peak assigned to the free OH stretch (3694 cm^{-1}) was assigned to have a phase of 0°. From the spectral fit, the uncoupled donor OH (3420 cm^{-1}) is found to have a phase of 180°. This phase difference agrees well with the respective projections of these bonds onto the surface normal, as the free OH should point on average, into the vapor phase, while the other OH oscillator must point toward the bulk phase to participate in significant hydrogen bonding. The phases of the two peaks assigned to tetrahedrally coordinated H_2O are the same as that found for the donor OH peak. By being 180° out of phase with the free OH peak, the phases of these two peaks imply an average molecular orientation for the tetrahedrally coordinated H_2O of the hydrogens pointing into the bulk liquid.

Figure 5 shows the resonant SF responses for the concentration series of HOD/H_2O/D_2O interfaces presented in Figure 2,

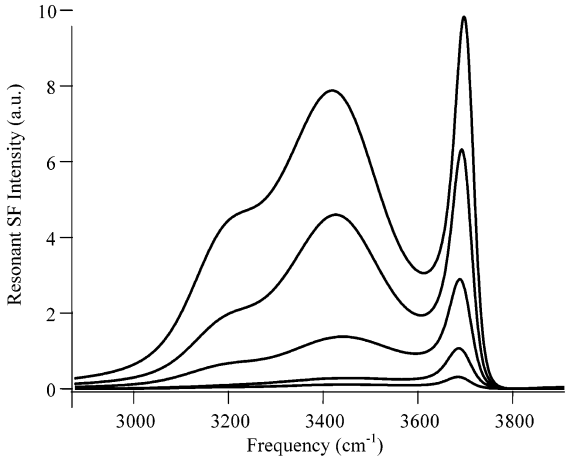

Figure 5. Resonant SF spectra of HOD/H_2O/D_2O mixtures, corresponding to the following equilibrium concentrations: (listed as mf H_2O, mf HOD, mf D_2O, from bottom to top). (a) 0.02 mf, 0.25 mf, 0.73 mf. (b) 0.08 mf, 0.41 mf, 0.51 mf. (c) 0.18 mf, 0.49 mf, 0.33 mf. (d) 0.51 mf, 0.41 mf, 0.08 mf. (e) 1.0 mf, 0 mf, 0 mf.

obtained by removing the nonresonant response from the fits to the data. Although interferences still arise between vibrational modes in these spectra, assigning a molecular interpretation is much more straightforward than when the resonant and nonresonant responses interfere with each other, as in the spectra of Figure 2. As the number of OH oscillators in the solution increases, the free OH mode at ~3700 cm^{-1} becomes more pronounced, as does the intensity at ~3420 cm^{-1}. From these resonant spectra, it is clear that the OH spectral features progressively grow in as the OH concentration increases toward pure H_2O, indicating that the interfacial hydrogen-bonding environment is not changing significantly as the OH concentration increases toward a pure vapor/H_2O interface.

The spectrum of the pure H_2O interface has been expanded in Figure 6b in the same manner as the HOD spectrum of Figure 4, with the resonant spectrum and its composite peaks depicted in Figure 6b. The intensity attributed to the tetrahedrally coordinated H_2O molecules in the interfacial region, peaks centered at 3200 cm^{-1} (± 10 cm^{-1}, Γ_ν = 80 cm^{-1} ± 10 cm^{-1}) and 3310 cm^{-1} (± 20 cm^{-1}, Γ_ν = 120 cm^{-1} ± 10 cm^{-1}), has grown significantly from the solution of 0.02 mf H_2O to the pure H_2O spectrum. The frequencies and widths of these peaks are coincident with spectral peaks observed in Raman and IR studies of room-temperature H_2O.[26−28] This coincidence is further confirmation that the hydrogen-bonding environment in the interfacial region is similar to that found in liquid H_2O. The donor OH has also increased in intensity, and has retained its frequency of 3420 cm^{-1}. While the predominant intensity in the 3420 cm^{-1} peak (± 10 cm^{-1}, Γ_ν = 100 cm^{-1} ± 15 cm^{-1}) is attributed to the uncoupled donor OH mode, tetrahedrally coordinated water molecules may also contribute to this intensity, as suggested by the intensity observed in IR and Raman studies of liquid H_2O.[26−28]

The free OH peak,[38] observed at 3694 cm^{-1} in the 0.25 mf HOD spectrum, shifts to the blue and gets narrower as the concentration of H_2O in the solution increases. These effects are in agreement with the work of Devlin, where the free OH of H_2O and HOD were observed to have different frequencies on ice surfaces, with the free OH of HOD molecules being shifted to the red of those occurring in H_2O molecules.[25,39] The observed narrowing of the free OH band in these studies is attributed to the existence of two unresolved free OH peaks, one from HOD at 3694 cm^{-1} and one from H_2O at 3706 cm^{-1}. As the concentration of H_2O in the interfacial region increases,

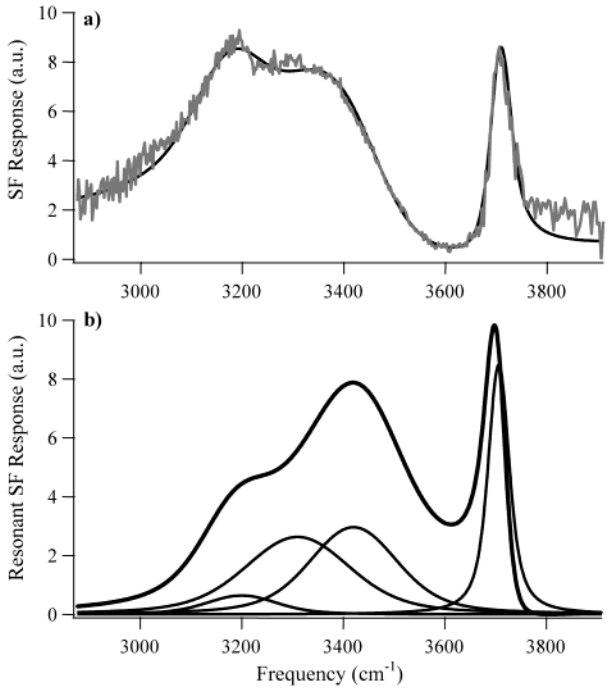

Figure 6. (a) Expanded pure H_2O spectrum with fit. (b) Resonant SF response from interfacial H_2O (thick solid line). The squared contributions from the different molecular species, $|\chi_\nu^{(2)}|^2$, are shown with thin solid lines.

the peak at higher frequency increases in intensity, while the HOD free OH peak decreases, thereby narrowing the band as the H_2O free OH peak becomes dominant as the solution composition approaches pure H_2O.

The resonant nonlinear susceptibility for each vibrational mode is proportional to the number of molecules contributing to the peak, and in the absence of molecular reorientation should track proportionally with the species concentration in the solution. The total susceptibility for each resonant peak, the quantity which is proportional to the number of contributing molecules, has been calculated by integrating each resonant $\chi_\nu^{(2)}$ (eq 3) over frequency. The result of this integral (henceforth described as the peak area) is proportional to $A_\nu\Gamma_\nu$, as defined in eq 3. The peak areas for each resonant mode are each then normalized to the corresponding peak area from the neat H_2O spectrum, and plotted as a function of species concentration. The peak areas are normalized in this way to remove the dependence on transition strength, which is larger for the more strongly hydrogen-bonded modes. The donor and free OH areas have been plotted as a function of the mole fraction (mf) of OH oscillators in solution (Figure 7a), while the areas of the peaks assigned to tetrahedrally coordinated H_2O (Figure 7b) are plotted as a function of the equilibrium mole fraction of H_2O. Also plotted are lines which represent the proportional relationship expected between the calculated number of contributing molecules (peak area) and the species concentration.

The number of free and donor OH oscillators obtained from the peak areas track very well with each other, as expected, as well as with the proportional relationship. The systematically higher value of the number of contributing species at high OH concentration for both the free and donor OH likely arises from the restriction in the phase relationship between these two peaks. The peak areas obtained for the tetrahedrally coordinated H_2O peak at 3310 cm^{-1} also agree well with the expected proportional relationship between the calculated number of molecules

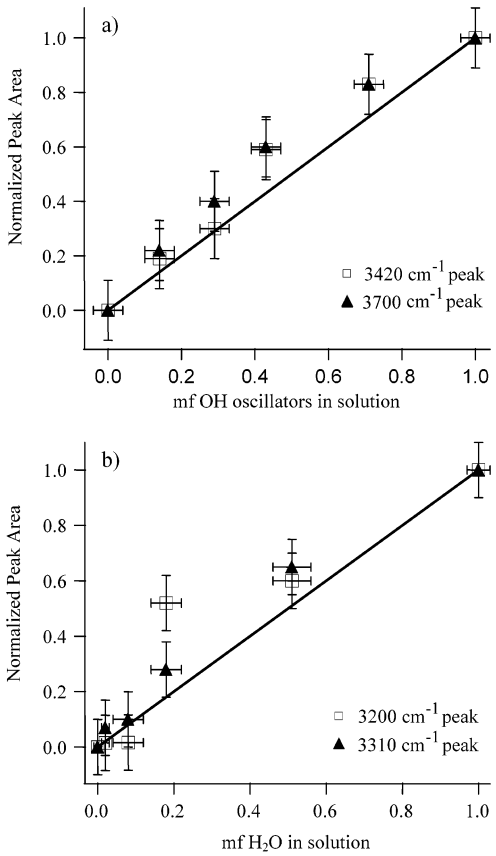

Figure 7. Normalized integrated $\chi_\nu^{(2)}$ for each of the four resonant peaks. (a) The areas for the free and donor OH species, (3420 and 3700 cm^{-1}, respectively) have been plotted as a function of the mole fraction (mf) of OH oscillators in the solution. (b) The areas for the two tetrahedral H_2O peaks (3200 and 3310 cm^{-1}) have been plotted as a function of the mf of H_2O in the solution.

and the concentration in solution. The areas of the 3200 cm^{-1} peak are also in good agreement, except for an anomalous departure at 0.18 mf H_2O. Overall, the quantitative agreement of the calculated peak areas, as a function of concentration, with the expected relationship provides confidence in the fitting routine used in these studies to deconvolve the concentration and assignment of different interfacial species.

Previous sum-frequency studies in this lab have investigated the hydrogen-bonding interactions at the interface between water and a hydrophobic interface, namely the CCl_4/H_2O interface.[40,41] These CCl_4/H_2O results have more recently been found to be similar at the dichloroethane/H_2O, dichloromethane/H_2O, and alkane/H_2O interfaces.[42,43] Although the measured spectra from these hydrophobic liquid/H_2O interfaces initially look quite different from the spectrum measured at the vapor/H_2O interface, which is also considered to be a hydrophobic interface, it is important to note that there is no detectable nonresonant SF contribution at these liquid/H_2O interfaces. When one compares only the resonant contribution of the vapor/H_2O SF spectrum to the SF spectrum of the CCl_4/H_2O interface (Figure 8), one finds that the general shape of the two spectra is much more similar than had been thought from previous studies, where the total vapor/H_2O spectrum was used to develop a molecular interpretation, rather than just the resonant response. Direct comparison of the two spectra reveals that the hydrogen-bonding interactions present at the two interfaces are not so dissimilar. The free-OH of the CCl_4/H_2O interface (3669 cm^{-1}) is slightly red shifted relative to that of the vapor/H_2O interface, due to the interaction of these OH oscillators with the CCl_4 phase, into

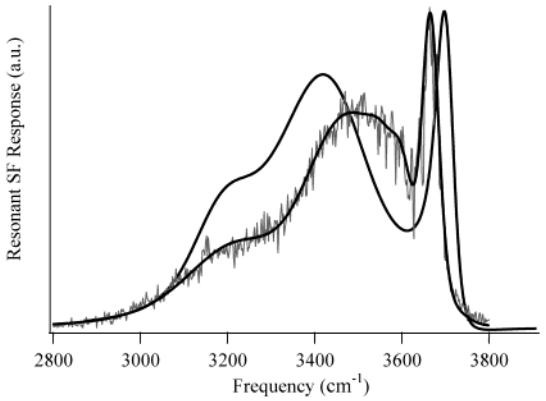

Figure 8. SF spectrum of the CCl_4/H_2O interface overlaid on the resonant spectrum of the vapor/H_2O interface. The CCl_4/H_2O spectrum is shown in gray with the best fit in black. The resonant vapor/H_2O spectrum is that of Figure 6b.

which they protude. The uncoupled donor OH mode at the CCl_4/H_2O interface is blue shifted $\sim$30 cm^{-1} from that occurring at the vapor/H_2O interface, indicating that these hydrogen bonds are weaker at the CCl_4/H_2O interface. This weakening in the hydrogen bonding is consistent with the lower surface tension of the CCl_4/H_2O interface of $\sim$46 mN/m as compared to $\sim$72 mN/m at the vapor/H_2O interface. Examining the 3200 cm^{-1} region of the two spectra, there is more relative intensity at lower frequencies in the vapor/H_2O spectrum than in the CCl_4/H_2O spectrum, indicating that among the tetrahedrally coordinated H_2O molecules in the interfacial region, there are stronger hydrogen-bonding interactions at the vapor/H_2O interface than at the CCl_4/H_2O interface, again consistent with surface tension measurements of the two interfaces.

MD Simulations

Although VSF spectra provide much information about the hydrogen-bonding environments present at a vapor/water interface, the information is not complete. The above discussion has been concerned with *ssp* spectra, which probe interfacial molecules with components of their dipole moment perpendicular to the interfacial plane. However, this is not a complete picture, as the remaining tensor components are not represented in the data. Experimentally, the dipole components parallel to the interfacial plane may be probed by obtaining *sps* spectra, but the signal levels are small,[22] relative to the *ssp* spectra. This lack of "in-plane" signal has two possible interpretations; either the interfacial molecules are oriented such that the components probed under *sps* polarization conditions are small, meaning the molecules are oriented largely perpendicular to the interfacial plane, or there is a large degree of cancellation of the "in-plane" components as a result of the randomness of the in-plane orientations, arising from the lack of orienting forces in the interfacial plane.

Fortunately, molecular dynamics simulations of the vapor/H_2O interface assist in providing information about the populations and orientations of these water molecules in the interfacial region that are isotropically distributed. MD simulations performed in the past decade have calculated a number of interfacial properties, including density profiles, molecular orientations, hydrogen-bonding strengths, and even IR spectra.[44−51] While many of these properties agree well with other experimental measurements, such as interfacial thicknesses from neutron and X-ray scattering experiments, they are often difficult to compare directly with sum-frequency spectra. Recently, however, a method for calculating sum-frequency spectra from MD simulations has been developed by Morita and Hynes.[9,10] This process of calculating sum-frequency spectra differs from the traditional calculation of IR spectra in that the tensor components (which are proportional to the IR and Raman transition moments) probed under the specific polarization conditions of interest are weighted by the orientation distributions of the interfacial molecules obtained from the MD simulations. Thus, as the water molecules in the simulation box become isotropic, the net orientational weighting is zero, and therefore the calculated nonlinear susceptibility is zero. Hydrogen-bond strengths are also obtained from the MD simulations, and used to distribute the SF intensity as a function of frequency. This simulation section primarily compares the experimental work discussed in the previous sections to the work of Morita and Hynes[9,10] (Figures 9 and 10). Two additional figures (Figures 11 and 12) generated from MD simulations performed in our laboratory, using the methods of Morita and Hynes, are included to further compare the simulations with the experimental data.

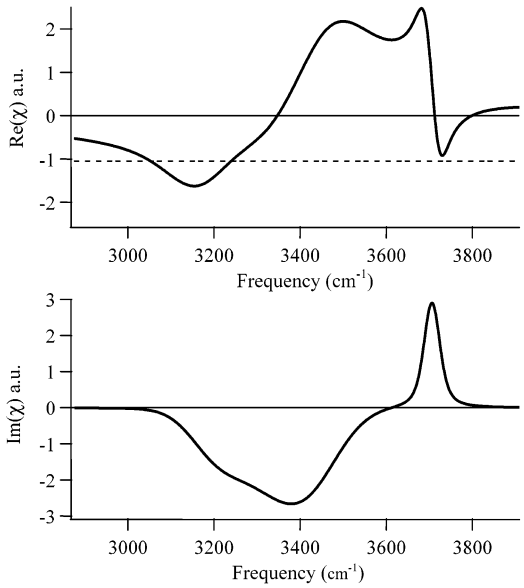

Figure 9. Real and imaginary components of $\chi^{(2)}$ obtained from the experimental resonant spectrum of the neat vapor/H_2O interface. The amplitude and sign of the nonresonant response used are shown with a dotted horizontal line.

The ability to separate the resonant and nonresonant SF responses at the vapor/H_2O interface has facilitated comparison of our experimental data (Figure 9) with the initial SF spectra calculated by Morita and Hynes, (Figure 10a), where the resonant response was calculated, but the nonresonant response was chosen such that the total spectrum resembled experimental data (nr $= -0.1$ au).[9] More recently, they have utilized a more rigorous calculation method and have been able to determine both the resonant and nonresonant nonlinear susceptibilities[10] (Figure 10b). Direct comparison of the real and imaginary pieces of the nonlinear susceptibility, $\chi^{(2)}(ssp)$, for a neat vapor/H_2O interface, obtained from both experiment (Figure 9) and from simulations (Figure 10a,b), reveals that the simulations are in quite good agreement with the experimentally measured responses. In particular, the free OH feature at 3700 cm^{-1} is well reproduced in the calculated susceptibilities, albeit somewhat broader than the experimental results, as is the negative peak in the imaginary component, corresponding to the donor OH at $\sim$3400 cm^{-1}. The calculated nonresonant susceptibility from the more rigorous calculations has approximately the same amplitude and the same sign (phase) as the nonresonant response measured experimentally.

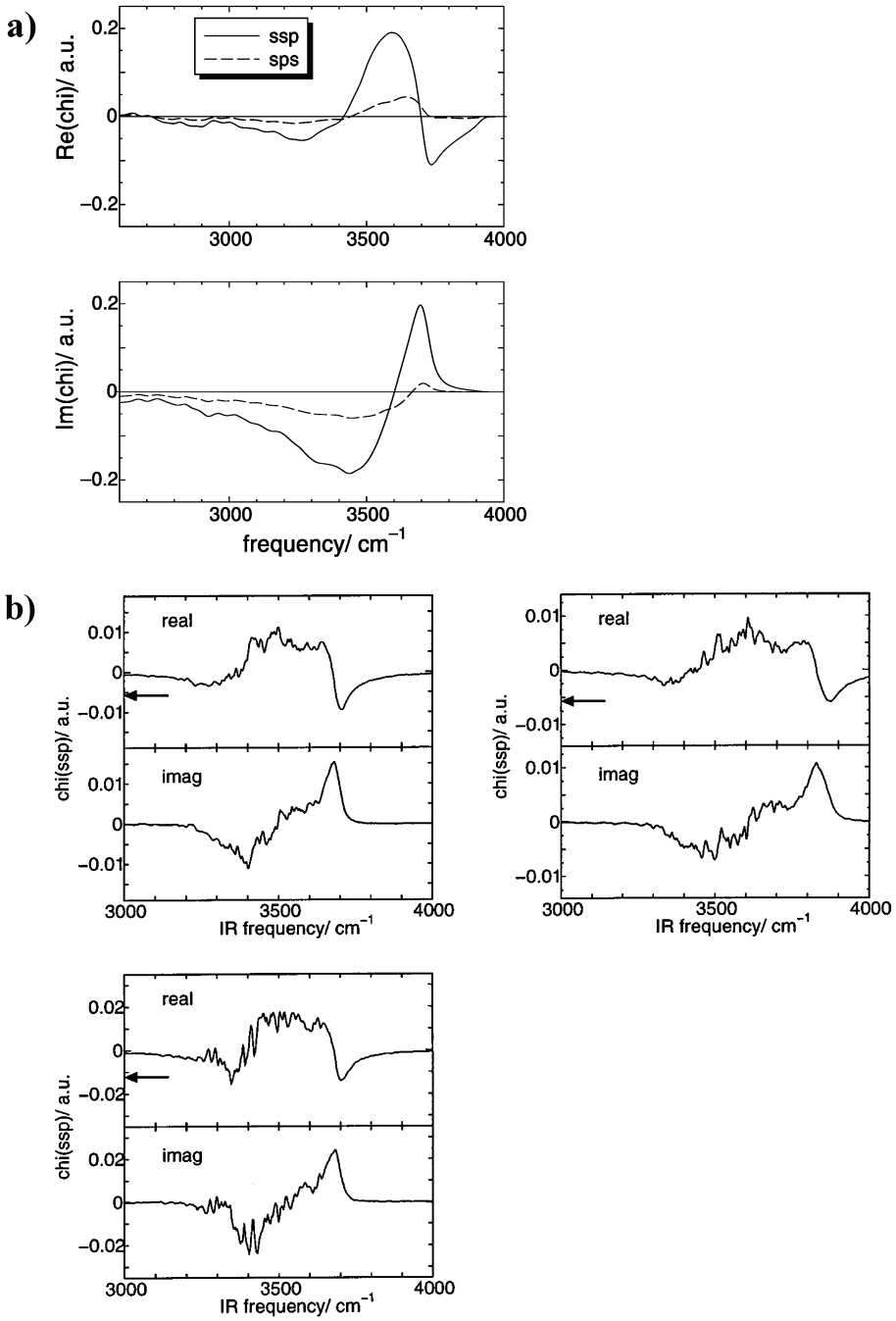

Figure 10. Real and imaginary components of $\chi^{(2)}$ obtained from the simulations performed by Morita and Hynes. (a) Plot of calculated real and imaginary components of $\chi^{(2)}$. Reprinted with permission from ref 9 copyright 2000, Elsevier. (b) Plots of calculated real and imaginary components of $\chi^{(2)}$ using a time dependent calculation approach, and three different potentials. The magnitude and sign of the calculated nonresonant response are shown with an arrow on each plot. Reprinted with permission from ref 10.

In addition to the calculation of SF spectra from interfaces, MD simulations can be used to investigate what molecular orientations and environments are contributing to the SF spectra, because due to the interferences that occur in the SF process, not all the molecules in the interfacial region contribute equally to a spectrum. Unlike most spectroscopic techniques, where the probe depth is determined by the wavelength of light used, how deeply into the material sum-frequency light is generated is determined by how deeply the molecules feel an orienting force induced by the presence of the interface. As mentioned before, as soon as the molecules become isotropic in their orientation, a net sum-frequency signal is no longer generated from these molecules.

MD simulations were performed in our lab to further investigate the types of molecules giving rise to an SF signal at a vapor/H_2O interface. These calculations were performed using the molecular dynamics package Amber, and utilized the SPC/E potential. The water box consists of 511 H_2O molecules and was run for 300 ps. Periodic boundary conditions were employed in three dimensions, and Ewald summation was used to calculate long-range forces. The process of generating the nonlinear susceptibilities for creating sum-frequency spectra closely follows the method developed by Morita and Hynes.[9,10]

Using the results of these simulations, the net resonant susceptibility was calculated as a function of distance along the water simulation box for the three distinct species in the

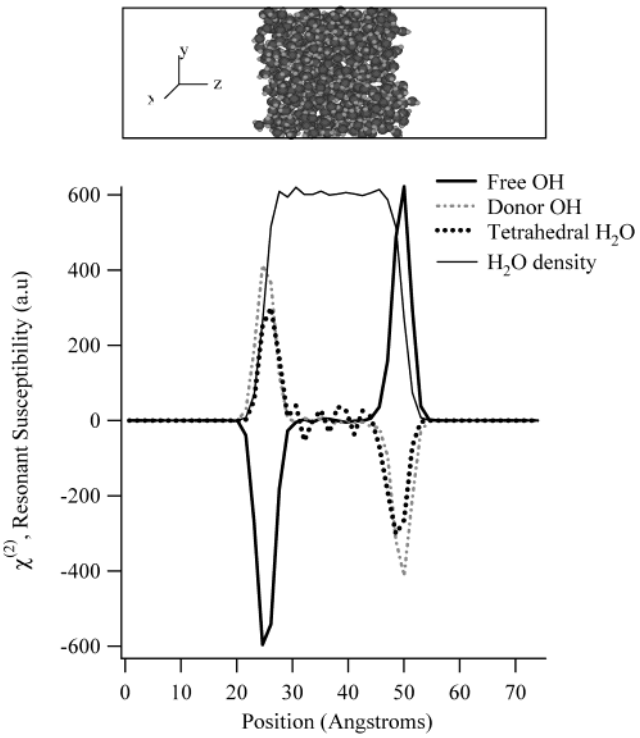

Figure 11. Plot of the resonant susceptibility as a function of distance along the simulation box (pictured above), for the three different molecular species: the free OH (solid black line), the uncoupled donor OH (grey dashed line), and H_2O molecules which participate in hydrogen bonding through both hydrogens (dashed black line). The density profile of the water slab has been overlaid on the plot as well.

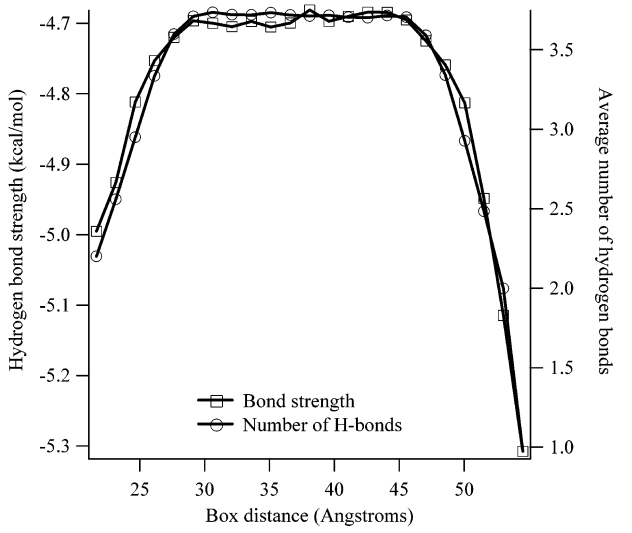

Figure 12. Plot of the average number of hydrogen bonds (circles, right axis) and average hydrogen bond strength (squares, left axis), obtained from MD simulation, as a function of distance along the simulation box.

interfacial region: the free OH, the uncoupled donor OH, and molecules which participate in at least two hydrogen bonds. The susceptibilities for these three species are plotted as a function of box distance in Figure 11, with the water density profile overlaid for reference. The reversal in sign of the peaks on the opposite sides of the water box reflects the fact that the air (vacuum) is toward negative *z* on the left side of the box, while it is in the direction of positive *z* on the right. This plot is a good first approximation of the interfacial depth as probed by sum-frequency spectroscopy. It is, however, only a first approximation, as no information about how the vibrational modes are distributed in frequency is accounted for in this calculation. Therefore, the interferences which occur due to overlapping vibrational modes are not represented in this figure. Several important features are evident from the plots of the nonlinear suceptibility as a function of distance, the first being that the susceptibility is only nonzero for a depth of ~10 Å. It is worth noting that this is the total distance over which the susceptibility is nonzero, and should not be directly compared to the interfacial thickness of ~3.3 Å obtained from X-ray scattering experiments,[52,53] which is defined as the root mean-square roughness of the interface.

The susceptibility arising from the free OH peaks slightly closer to the vapor phase than the susceptibility from the other two species, which is expected, as the free OH protrudes on average into the vapor phase, while the peak from the hydrogen-bonded H_2O extends the furthest toward the bulk H_2O, also as expected. The opposite sign of the net free OH susceptibility indicates that it has the opposite phase, and is therefore pointed on average in the opposite direction from both the uncoupled donor OH and hydrogen-bonded H_2O moieties, in agreement with what is observed in experiments, and what has been calculated by previous MD simulations.[44−51] The free OH susceptibility is significantly larger than the susceptibilities of the other two species, which arises in part from the large amount of orientationally induced cancellation that occurs for the donor OH and hydrogen-bonded H_2O, as their average orientations have a larger component in the plane of the interface than the free OH orientation does. The change in dipole transition strength as a function of hydrogen bonding has not been included in the calculation at this point, which also accounts for the large relative susceptibility of the free OH, as the susceptibilities of the hydrogen-bonded species increase in magnitude upon participation in hydrogen bonding.

One of the most significant conclusions arising from the MD simulation calculations is that sum-frequency is a more sensitive probe of the uncoupled free and donor OH stretching modes than of the tetrahedrally coordinated water molecules in the interfacial region. This selectivity arises from the preferential orientation of the tetrahedral molecules toward the plane of the interface. In the case of the tetrahedrally coordinated H_2O molecules, the molecules are oriented primarily in the plane of the interface with their hydrogens pointed only slightly toward the bulk H_2O. The lack of strong orienting forces within the interfacial plane results in a large degree of cancellation of sum-frequency signal from these molecules. As mentioned previously, spectra of the vapor/H_2O interface taken under *sps* polarization conditions show very little intensity in the OH stretching region. From the orientations obtained from MD simulations, this lack of signal should be attributed to the cancellation of SF light, and not to the predominance of molecules oriented perpendicular to the interfacial plane. It is important to reiterate that due to this cancellation, less information is obtained from the sum-frequency spectra about the hydrogen-bonding interactions occurring in the interfacial plane relative to out of the plane.

From the molecular dynamics simulations, it is possible not only to analyze the molecular orientations, but also to characterize the molecular interactions in the interfacial region. Two important questions that the simulations can answer are: How do the number and strength of hydrogen bonds change as you approach the interface? Figure 12 shows both the average number of hydrogen bonds per H_2O molecule, as well as the average hydrogen bond strength as a function of box distance. (The number of hydrogen bonds was determined by counting

the number of hydrogens (on other water molecules) within a radius of 2.5 Å from each water molecule's oxygen. The hydrogen bond strength is determined by calculating the potential energy between molecules.) As the interface is approached, the number of hydrogen bonds decreases, as expected from the presence of free OH oscillators. However, as the number of hydrogen bonds decreases, the average hydrogen bond strength increases. This result is quite significant, as both the experimental and simulated sum-frequency spectra show intensity at frequencies similar to that found in bulk spectra of liquid H_2O. What can be inferred then, is that although the hydrogen bonding is becoming stronger in the interfacial region, the hydrogen-bonding environment is still more similar to that of liquid H_2O than to ice, due to the decrease in the number of hydrogen bonds.

Given the similarity of the calculated nonlinear susceptibilities (both resonant and nonresonant) to the susceptibilities obtained from the experimental data, it appears that simulations of sum-frequency spectra at interfaces will be a valuable tool with which to complement experimental results. The ability to directly compare sum-frequency spectra with simulated spectra allows the further development of our understanding of the molecular species and their hydrogen-bonding character at the interface as well as improved developments of models which more accurately represent the H_2O-H_2O interactions at a surface.

Conclusions

While the total sum-frequency spectrum obtained for the vapor/H_2O interface is consistent with spectra obtained from previous studies,[22] the conclusions drawn from this work about the interfacial hydrogen-bonding environment significantly advance the understanding of the hydrogen-bonding character of interfacial water molecules beyond what was previously known. The studies presented here use isotopic dilution experiments to simplify the OH stretching region of the spectrum, and are therefore able to explore more thoroughly the interfacial hydrogen bonding. The measurement of the nonresonant response from a neat D_2O interface allows the resonant and nonresonant sum-frequency responses to be separated, so that the interpretation of the interfacial molecular interactions is based only on the resonant sum-frequency response. The resonant spectrum of a primarily HOD/D_2O interface allows the assignment of a peak due to the uncoupled donor OH oscillators, the first assignment from SF studies of the hydrogen-bonded OH of molecules which straddle the vapor/water interface. The hydrogen-bonding environment suggested by the frequency of this vibrational mode is consistent with that found in bulk liquid studies. By obtaining spectra of other mixtures of HOD, H_2O, and D_2O, the peak fit parameters were constrained, enabling a consistent set of fits to the spectra to be obtained. From the resonant spectrum of the pure/H_2O interface, in addition to the free OH, the predominant intensity is in the 3400 cm^{-1} region of the spectrum, with a lesser contribution in the 3200−3300 cm^{-1} region. This observed resonant intensity is much more consistent with the intensity observed in IR and Raman studies of room-temperature liquid water than with studies of ice, where the predominant intensity is centered at ∼3150 cm^{-1}. Quantitative comparison of the sum-frequency response as a function of species concentration shows good agreement between the free and donor OH signal, both with the number of OH oscillators in the solution, and with each other. The signal from the tetrahedrally coordinated H_2O also tracks well with the concentration of H_2O in the solution, indicating that four resonant peaks model well the vibrational modes in the interfacial region.

Comparison of the resonant SF spectrum of the vapor/H_2O interface with that of the CCl_4/H_2O interface reveals a greater similarity between the two interfaces than previous work would suggest. Although the hydrogen-bonding interactions between water molecules at the CCl_4/H_2O are weaker than those occurring at the vapor/H_2O interface, in agreement with the decreased surface tension of the CCl_4/H_2O interface, the overall bonding environment at both interfaces seems to be much more characteristic of those found in liquid water than in ice. It is important to remember that the SF spectra presented here, both simulated and experimental, are taken under *ssp* polarization conditions, which probes only one of the 7 nonzero tensor elements for the interfacial molecules. More specifically, only molecules with a component of their dipole moment perpendicular to the interfacial plane contribute to the sum-frequency spectra presented here, so those molecules which are oriented in the interfacial plane and which may have much stronger hydrogen bonding are not reflected in these studies.

Recent calculations of the sum-frequency spectra at a vapor/H_2O interface have shown good agreement with experimental spectra, given the approximate nature of the description of H_2O-H_2O interactions. From these simulations, it is possible to extract information about the interactions and orientations of water molecules in the interfacial region, as well as to calculate an approximate interfacial thickness probed by sum-frequency. Profiles of the nonlinear susceptibility as a function of simulation box distance indicate the majority of the sum-frequency intensity arises from the top ∼6 Å of water, while there is no net sum-frequency intensity after ∼10 Å.

The combination of isotopic dilution SF experiments and molecular dynamics simulations have provided a more detailed and complete picture of the hydrogen-bonding environment experienced by water molecules at the vapor/H_2O interface. Both the experimental and calculated spectra show significant intensity that is consistent with spectra of bulk liquid H_2O. The MD simulations provide detailed information about the actual distribution of interfacial molecules, as well as how much each orientation contributes to the SF spectrum. Further MD simulations are in progress to examine and compare the experimental sum-frequency results with other H_2O-H_2O interaction models.

Acknowledgment. The authors thank the National Science Foundation, (CHE-9725751) and the Petroleum Research Fund of the American Chemical Society for support of this work. E.A.R. also acknowledges the support of the NSF IGERT program.

References and Notes

(1) Buck, M.; Himmelhaus, M. *J. Vac. Sci. Technol. A* **2001**, *19*, 2717.
(2) Miranda, P. B.; Shen, Y. R. *J. Phys. Chem. B* **1999**, *103*, 3292.
(3) Richmond, G. L. *Annu. Rev. Phys. Chem.* **2001**, *52*, 357.
(4) Shultz, M. J.; Baldelli, S.; Schnitzer, C.; Simonelli, D. *J. Phys. Chem. B* **2002**, *106*, 5313.
(5) Du, Q.; Superfine, R.; Freysz, E.; Shen, Y. R. *Phys. Rev. Lett.* **1993**, *70*, 2313.
(6) Du, Q.; Freysz, E.; Shen, Y. R. *Science* **1994**, *264*, 826.
(7) Raduge, C.; Pflumio, V.; Shen, Y. R. *Chem. Phys. Lett.* **1997**, *274*, 140.
(8) Raymond, E. A.; Tarbuck, T. L.; Richmond, G. L. *J. Phys. Chem. B* **2002**, *106*, 2817.
(9) Morita, A.; Hynes, J. T. *Chem. Phys.* **2000**, *258*, 371.
(10) Morita, A.; Hynes, J. T. *J. Phys. Chem. B* **2002**, *106*, 673.
(11) Bain, C. D.; Davies, P. B.; Ong, T. H.; Ward, R. N.; Brown, M. A. *Langmuir* **1991**, *7*, 1563.
(12) Bloembergen, N.; Pershan, P. S. *Phys. Rev.* **1962**, *128*, 606.
(13) Dick, B.; Gierulski, A.; Marowsky, G. *Appl. Phys. B* **1985**, *38*, 107.
(14) Shen, Y. R. *The principles of nonlinear optics*, 1st ed; John Wiley & Sons: New York, 1984.

(15) Lobau, J.; Wolfrum, K. *J. Opt. Soc. Am. B* **1997**, *14*, 2505.
(16) Woutersen, S.; Emmerichs, U.; Bakker, H. J. *Science* **1997**, *278*, 658.
(17) Nienhuys, H. K.; van Santen, R. A.; Bakker, H. J. *J. Chem. Phys.* **2000**, *112*, 8487.
(18) Brown, M. G.; Raymond, E. A.; Allen, H. C.; Scatena, L. F.; Richmond, G. L. *J. Phys. Chem. A* **2000**, *104*, 10220.
(19) Allen, H. C.; Raymond, E. A.; Richmond, G. L. *J. Phys. Chem. A* **2001**, *105*, 1649.
(20) Gragson, D. E.; McCarty, B. M.; Richmond, G. L.; Alavi, D. S. *J. Opt. Soc. Am. B* **1996**, *13*, 2075.
(21) *CRC handbook of lasers, with selected data on optical technology*; Pressley, R. J., Ed.; Chemical Rubber Co.: Cleveland, 1971.
(22) Wei, X.; Shen, Y. R. *Phys. Rev. Lett.* **2001**, *86*, 4799.
(23) Bertie, J. E.; Ahmed, M. K.; Eysel, H. H. *J. Phys. Chem.* **1989**, *93*, 2210.
(24) Bertie, J. E.; Lan, Z. *Appl. Spectrosc.* **1996**, *50*, 1047.
(25) Devlin, J. P. *J. Chem. Phys.* **2000**, *112*, 5527.
(26) Scherer, J. R. The Vibrational Spectroscopy of Water. In *Advances in Infrared and Raman Spectroscopy*; Clark, R. J. H., Hester, R. E., Eds.; Heyden: Philadelphia, 1978; Vol. 5.
(27) Walrafen, G. E. Raman and Infrared Spectral Investigations of Water Structure. In *Water: A Comprehensive Treatise*; Franks, F., Ed.; Plenum Press: New York, 1972; Vol. 1, Chapter 5.
(28) Walrafen, G. E.; Hokmabadi, M. S.; Yang, W.-H. *J. Chem. Phys.* **1986**, *85*, 6964.
(29) Wojcik, M. J.; Buch, V.; Devlin, J. P. *J. Chem. Phys.* **1993**, *99*, 2332.
(30) Buck, U.; Ettischer, I.; Melzer, M.; Buch, V.; Sadlej, J. *Phys. Rev. Lett.* **1998**, *80*, 2578.
(31) Pribble, R. N.; Zwier, T. S. *Science* **1994**, *265*, 75.
(32) Gruenloh, C. J.; Carney, J. R.; Hagemeister, F. C.; Arrington, C. A.; Zwier, T. S.; Fredericks, S. Y.; Wood, J. T.; Jordan, K. D. *J. Chem. Phys.* **1998**, *109*, 6601.
(33) Devlin, J. P.; Sadlej, J.; Buch, V. *J. Phys. Chem. A* **2001**, *105*, 974.
(34) Hare, D. E.; Sorensen, C. M. *J. Chem. Phys.* **1990**, *93*, 6954.
(35) Ritzhaupt, G.; Collier, W. B.; Thornton, C.; Devlin, J. P. *Chem. Phys. Lett.* **1980**, *70*, 294.
(36) Wilson, E. B.; Pimentel, G. C. *The hydrogen bond*; W. H. Freeman: San Francisco, 1960; Chapter 3.
(37) Huggins, C. M.; Pimentel, G. C. *J. Phys. Chem.* **1956**, *60*, 1615.
(38) All listed free OH frequencies have an uncertainty of ± 5 cm^{-1}. The peak widths (± 3 cm^{-1}) and frequencies for spectra b−f in Figure 2 are the following: (b) 24 cm^{-1}, 3694 cm^{-1}; (c) 24 cm^{-1}, 3694 cm^{-1}; (d) 22 cm^{-1}, 3698 cm^{-1}; (e) 19 cm^{-1}, 3701 cm^{-1}; (f) 19 cm^{-1}, 3706 cm^{-1}.
(39) Rowland, B.; Fisher, M.; Devlin, J. P. *J. Chem. Phys.* **1991**, *95*, 1378.
(40) Scatena, L. F.; Brown, M. G.; Richmond, G. L. *Science* **2001**, *292*, 908.
(41) Scatena, L. F.; Richmond, G. L. *J. Phys. Chem. B* **2001**, *105*, 11240.
(42) Brown, M. G.; Walker, D. S.; Richmond, G. L. *J. Phys. Chem. B*, in press.
(43) Brown, M. G.; Walker, D. S.; Richmond, G. L. In Preparation.
(44) Dang, L. X.; Chang, T. M. *J. Chem. Phys.* **1997**, *106*, 8149.
(45) Matsumoto, M.; Kataoka, Y. *J. Chem. Phys.* **1988**, *88*, 3233.
(46) Motakabbir, K. A.; Berkowitz, M. L. *Chem. Phys. Lett.* **1991**, *176*, 61.
(47) Sokhan, V. P.; Tildesley, D. J. *Mol. Phys.* **1997**, *92*, 625.
(48) Taylor, R. S.; Dang, L. X.; Garrett, B. C. *J. Phys. Chem.* **1996**, *100*, 11720.
(49) Townsend, R. M.; Rice, S. A. *J. Chem. Phys.* **1991**, *94*, 2207.
(50) Wilson, M. A.; Pohorille, A.; Pratt, L. R. *J. Phys. Chem.* **1987**, *91*, 4873.
(51) Wilson, M. A.; Pohorille, A.; Pratt, L. R. *J. Chem. Phys.* **1988**, *88*, 3281.
(52) Braslau, A.; Deutsch, M.; Pershan, P. S.; Weiss, A. H.; Als-Nielsen, J.; Bohr, J. *Phys. Rev. Lett.* **1985**, *54*, 114.
(53) Braslau, A.; Pershan, P. S.; Swislow, G.; Ocko, B. M.; Als-Nielsen, J. *Phys. Rev. A* **1988**, *38*, 2457.